International Journal of Computing Academic Research (IJCAR)
ISSN 2305-9184, Volume 5, Number 2 (April 2016), pp.110-121

http://www.meacse.org/ijcar

Use of a Tin (Sn) Flat Sheet as a Material Filter for Reduction of Scattered Gamma Photons and Enhancement of Cold Regions Image Quality in Tc-99m SPECT

Inayatullah Shah Sayed

Department of Medical Engineering and Physics, King's College Hospital (Dulwich), Guy's King's and St. Thomas School of Medicine, University of London, UK
Present address: Department of Diagnostic Imaging and Radiotherapy, Kulliyyah of Allied Health Sciences, International Islamic University Malaysia, Kuantan Campus, 25200 Kuantan, Pahang, Malaysia

Abstract

The presence of scattered gamma photons in SPECT data degrade the quality of reconstructed images. In this work, a material filter was employed in order to improve cold regions detectability and overall image quality by pre-filtering of some fraction of scattered gamma photons. Material filter was constructed from a 300x300mm flat sheet of tin (Sn) 0.25mm thick. It was installed on the outer surface of LEGP collimator of a gamma camera. Tc-99m spectra were plotted from the count rates recorded without and with material filter by scanning a cylindrical source tank in contiguous 10 keV energy windows (55-65, 65-75,……155-165 keV). SPECT image data of R. A. Carlson's phantom with cold regions insert (placed into the cylindrical tank) were gathered without and with material filter by setting 20% energy window centered at 140 keV. Images were reconstructed by applying filtered back projection method. Tc-99m spectra show the reduction in count rate with material filter from the lower part of the photopeak region <132 keV. Significant decrease in %RMS noise, enhancement of cold regions detectability and significant improvement in contrast of cold regions of diameter 7.3, 9.2 and 11.4 mm at $p < 0.05$, but, statistically insignificant improvement in contrast of 5.9, 14.3 and 17.9 mm diameter cold regions was achieved with material filter. Findings show that the material filter removes some fraction of scattered gamma photons from image data. Thus, improves SPECT image quality. However, further investigations under clinically realistic conditions require.

Keywords: Scatter reduction, Material filter, Contrast enhancement, SPECT image quality

Introduction

In order to diagnose diseases both visual interpretation and semi-quantitative analysis of SPECT images are performed and the accuracy of clinical investigations is well influenced by the quality of images. In this modality, gamma emitting radionuclides (typically, Tc-99m with gamma - energy of 140 keV) are used, and the dominant interaction process within the patient is Compton scattering. It is commonly appreciated that the presence of Compton scattered gamma photons decrease the image contrast and lead to an overall degradation in the perceived quality of the reconstructed image [1–10]. Attempts to correct for such effects are an ongoing activity [11–15] with a view to improve the quantitative accuracy and quality of images. A simple approach, asymmetric energy window [16] was used to eliminate the scattered gamma photons by raising the low level of pulse height analyzer. The disadvantage with this method is the reduction of some un-scattered photon counts from the image data. Hence the decrease in SNR as compared to 20% symmetric energy window [17, 18]. Another method is based on calculation of scatter fraction and then subtraction of that fraction from the image data [19, 20]. Also,

other approaches, such as, dual and triple energy window subtraction were developed by [21–25]. In dual energy window methods, data are collected in scatter and photopeak energy windows. The data collected in the photopeak energy window are corrected by subtracting scatter energy window data. A channel ratio method [25] corrects the effects of scatter in SPECT by dividing a photopeak symmetrically into two adjacent energy windows and the observed change in the ratio of the counts is obtained and used. In addition, a simple way to reduce the scatter effects from the SPECT images exists, which is the use of an effective attenuation coefficient (0.12/cm) rather than the actual value i.e., 0.15/cm for Tc-99m in water. However, every method has some limitations.

Muehllehner and Jaszczak [26] used composite filters (material filters) to reduce the recording of undesirable (scattered) photons from the photopeak region of Tc-99m spectrum. Pillay and his colleagues [27] applied an alloy filter consisting of Pb, Zn and Sn in single photon emission (planar) imaging and report the enhancement in the image contrast of various patient studies suggested the possibility of employing the technique in SPECT. Another alloy filter consisting of Cd and Cu materials for gamma ray camera was developed by [28]. Pollard [29] employed lead sheets (1.6mm - 6.4mm) as material filters and attached on the front face of a gamma camera for scanning therapeutic doses of I-131. Furthermore, a Monte Carlo study was done by the same group simulating their experimental setup and found that system resolution is degraded by the Pb sheet. Lead filters were also used by Spinks and Shah [30] in order to remove the number of Compton scattered events recorded in PET scanning. Moreover, Shah [31] investigated the effects of Sn material sheet 0.25mm thick on spatial resolution and uniformity in Tc-99m imaging and reported improvement with the technique.

This study aimed to remove some fraction of scattered gamma photons with a material filter tin (Sn) from SPECT data in order to enhance the cold regions image quality. Tc-99m spectra without and with material filter were analyzed in terms of reduction in count rates, particularly, from the lower part of photopeak where majority of scatter gamma photons is present. Reconstructed images of cold regions were investigated with respect to regions detectability, %RMS noise and contrast.

Methods and Materials

Construction of Tin (Sn) material filter

In SPECT imaging, Tc-99m is very widely used. Thus, the material filter from a thin flat sheet of tin (Sn) was constructed only for gamma photon energy of 140 keV as shown in Fig. 1. The tin (Sn) material as a filter was chosen from copper (Cu), lead (Pb) and tungsten (W) on the basis of calculated results of fractional absorption of different gamma photon energies, i.e., 50 - 150 keV as shown in (Fig. 2). It shows that both Cu and Sn appear to be suitable candidates for filter material. However, overall Sn attenuates comparatively more photons than Cu at low energies ranging from 125 to 135 keV (wider shaded area in Fig. 2). It should be noted that in Tc-99m single photon emission imaging the width of 20% symmetrical energy window ranges 125 to 154 keV. The decision on the suitable thickness of the filter for Tc-99m photons was made on the results of theoretical calculations on percent attenuation of a range of gamma photon energies by different thicknesses.

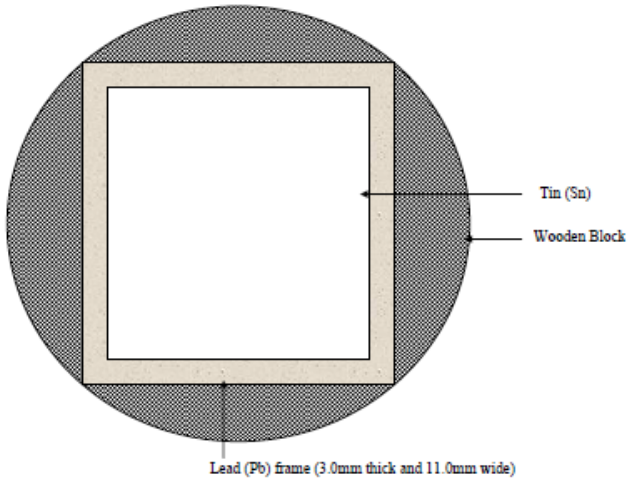

Fig. 1 Construction of material filter from a flat sheet of tin (Sn).

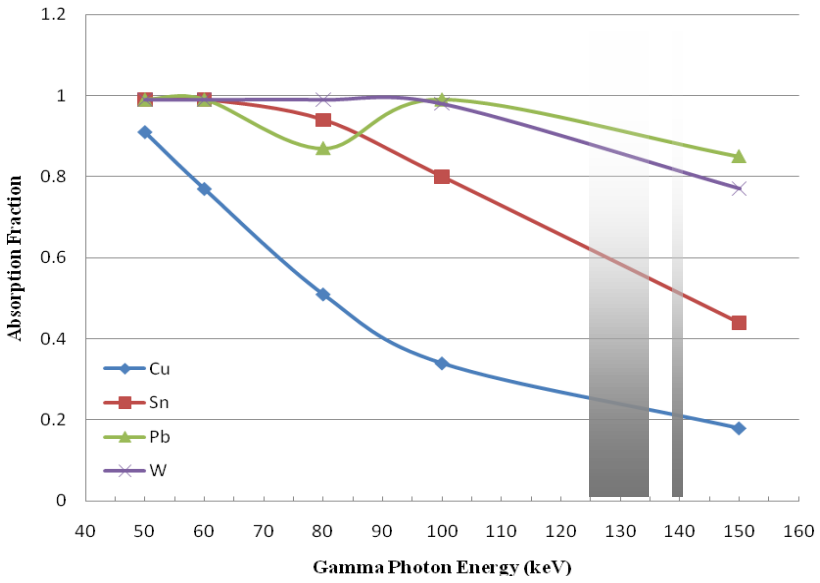

Fig. 2 Show the absorption fraction of different gamma photon energies (50 - 150 keV) by different materials.

Measurement of energy spectra of Tc-99m in scattering medium without and with material filter

Data for energy spectra of Tc-99m radionuclide were obtained by using a GE400 AC/T scanning unit. Water filled and uniformly distributed radioactivity in the cylindrical acrylic phantom of inner diameter 20.32 cm and length 31.00 cm (Carlson phantom with no inserts) without and with a 0.25 mm tin (Sn) material filter was scanned. Material filter was mounted on the outer surface of low energy general purpose (LEGP) collimator. Phantom was positioned in the centre of the field of view with its long axis parallel to the surface of the collimator. The position of the gamma camera and phantom remained unchanged throughout the two sets of

measurements. Image matrix size was chosen at 64x64x16. Count rates were recorded in contiguous 10 keV energy windows (two minutes/window) spanning 55 - 165 keV and corrected for decay. The spectra of relative count rates versus energy window threshold were plotted as shown in Fig. 3.

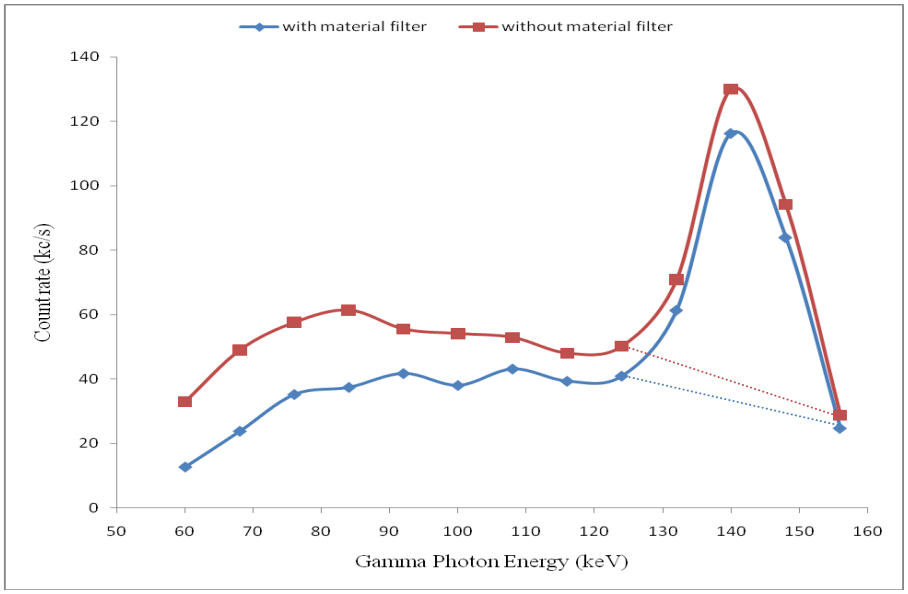

Fig. 3 Energy spectra of Tc-99m radionuclide in scattering medium, without and with material filter.

SPECT data acquisition and image reconstruction without and with material filter

A Tc-99m filled Carlson phantom was used, but, in this case with an acrylic insert to simulate cold regions in a hot background. The insert consisted of seven acrylic rods with diameters 5.9, 7.3, 9.2, 11.4, 14.3, 17.9 and 22.4mm, schematic cross-sectional view of insert is shown in (Fig. 4). Data were collected without and with material filter within a 20% symmetric photopeak energy window (126 - 154 keV) centered at 140 keV. Gamma camera (GE400 AC/T) installed with LEGP collimator was used and 128x128x16 imaging matrix was selected. Sixty four views (30 sec/view) were taken over 360^{O} and cross-sectional images were produced by filtered backprojection technique. A 5^{th} order Butterworth filter with 0.30 cycles/cm cut-off frequency was chosen. Chang's attenuation correction technique [33] was employed. The actual value of the attenuation coefficient (0.151/cm) for Tc-99m in water was applied to the data in the case where material filter was mounted and an effective attenuation coefficient (EAC) value 0.121/cm [24] was chosen where no material filter was employed. This choice of attenuation coefficients represents a more severe test of the material filter, since it presupposes that all scattered gamma photons are selectively removed by the material filter.

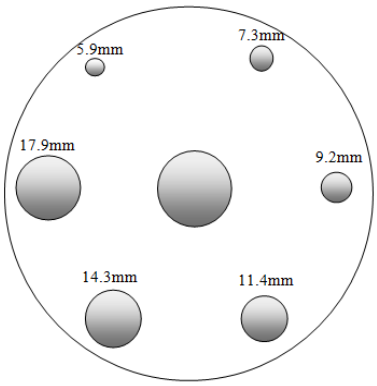

Fig. 4 Cross sectional view of cold regions insert of Carlson's phantom.

Percent root mean square noise (%RMS noise)

Reconstructed images obtained from without and with material filtered data were retrieved/displayed and analyzed by applying ImageJ software [34] to calculate and compare the noise level in the count density of the transverse image background. To investigate the effect of material filter on %RMS noise in the transverse image background an irregular large ROI was drawn and placed carefully avoiding the overlapping of cold regions. This measurement provides an estimate of the presence of noise component in the image. Eq. 1 is applied to calculate %RMS noise [35]. Statistical analysis was performed by using one-way ANOVA test to evaluate the difference between %RMS noise values.

$$\%RMSnoise = \frac{SD}{D_{mean}} \quad (1)$$

where SD is the standard deviation of the average count density / pixel in ROI and D_{mean} is the average count density / pixel in ROI.

Cold region contrast measurement

In order to measure the contrast different regions of interest (ROI) were drawn according to the size of each cold region and carefully placed within the boundaries of cold region for numerical analysis. These ROIs were copied (separately) on the computer clip board and pasted on the next image, so that the size of the ROI for each cold region remained consistent for images obtained without and with the material filter. Background counts were determined by drawing a larger irregular ROI over the entire image, but, avoiding the known locations of cold regions. Eq. 2 was applied for the calculation of cold region contrast (C_{CR}).

$$C_{CR} = \frac{D_{region} - D_{bkg}}{D_{bkg}} \quad (2)$$

where D_{region} is the count density in the region and D_{bkg} is the count density in the background.
Errors, E_{CR} in contrast values were calculated from the Eq. 3.

$$E_{CR} = C_{CR}\sqrt{\frac{EA^2 + EB^2}{(A-B)^2} + \frac{EB^2}{B^2}} \quad (3)$$

Where C_{CR} represents the measured cold region image contrast, A and B indicate the average count densities in the area of interest in the cold region and in the background, respectively. EA and EB are the error (standard deviation) in A and B, respectively.

Statistical analysis was done on the measured contrast values obtained from without and with material filtered data by applying *t* test in order to calculate the significant difference between the contrast values of two sets.

Results

Energy spectra of Tc-99m

A marked reduction in the count rate from the scatter part as well as some decrease from photopeak region of energy spectrum of Tc-99m with material filter was recorded. However, decrease in the count rate from photopeak region can be considered due to the absorption of some fraction of both scattered and primary gamma photons by material filter. On average 12.61% decrease in the count rate of gamma photon energies ranging from 125 – 155 keV of the Tc-99m energy spectrum was measured. In addition, 35% reduction in count rate (average) of low energy (scattered) gamma photons ranging 60 - 125 keV was observed. For detailed analysis of photopeak, count rate data were plotted using MS Excel software. Fig. 5, shows a substantial reduction in the relative count rate of gamma photon energies of 125, 130 and 135 keV which is 19.3%, 14.3% and 10.7%, respectively.

However, for 140, 145 and 150 keV gamma photon energies, 10.8%, 10.6% and 10% decrease, respectively in the count rate was recorded with the material filter. In this part of research focus is given to the photopeak region, because images are produced from the data of this region only.

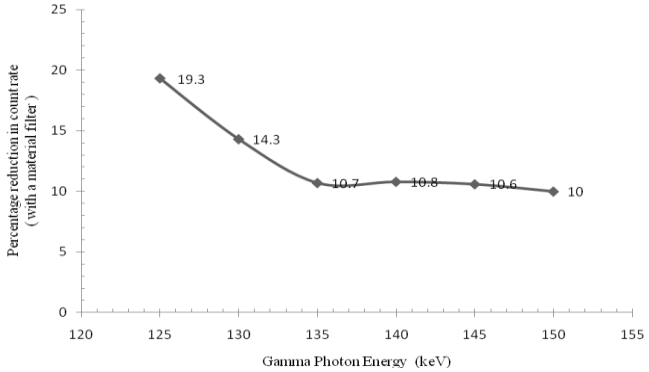

Fig. 5 Percentage reduction in count rate with material filter as compared to without material filter from the region 125 - 150 keV of Tc-99m spectrum (radioactivity in scattering medium)

Percent root square mean noise (%RMS noise)

SPECT image quality is analyzed by various parameters, e.g., estimation of %RMS noise. One of the sources of noise in image is the presence of scattered gamma photons in image projection data. Investigations into the

material filtered data shows significant ($p<0.05$) decrease in %RMS noise shown in Table 1 (measurements were repeated three times).

Table 1. Show the %RMS noise values of transverse image without and with material filter

%RMS noise	
Without material filter	With material filter
41.33 +/- 0.577	29.66 +/- 0.577

Cold regions detectability and contrast

Generally, in diagnostic imaging emphasis is placed on the detection of abnormalities by differentiating lesions from background. This task is made more difficult when the contrast is lower between the lesion and background. Furthermore, the accuracy in the diagnosis of disease depends upon image quality. In this paper the potential advantage of the material filter as compared to without material filter (use of an effective linear attenuation coefficient value) was assessed in terms of detectability and contrast of cold regions. Images (Fig. 6a and b) were displayed by selecting similar image display parameters for without and with material filtered images. Reconstructed transverse image obtained with material filtering showed smaller cold regions clearer relative to the image produced from the data acquired without material filter (Fig. 6a and b).

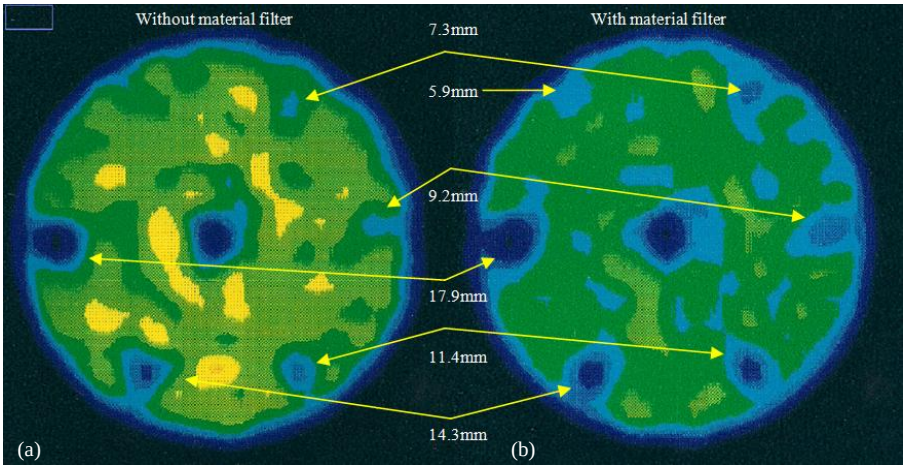

Fig. 6 Transverse image slices of cold regions insert of Carlson's phantom (a) without and (b) with material filter with LEGP collimator.

Contrast values (Fig. 7) measured from images obtained with a material filter were compared with those images obtained without the use of a material filter by employing a simple scatter correction technique, i. e., use of an effective attenuation coefficient value 0.121/cm. These contrast values are negative but the sign has been ignored. Significant improvement in image contrast was achieved by material filter technique for cold regions of diameter 11.4, 9.2 and 7.3mm. However, results of cold regions contrast having diameters larger than 11.4 mm were equivocal.

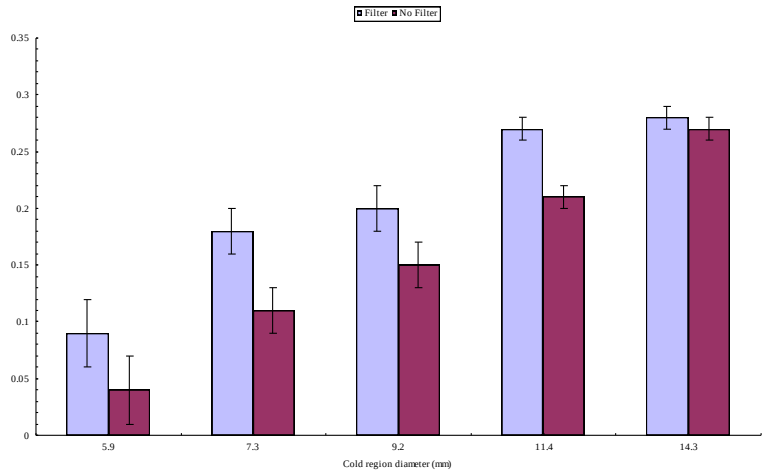

Fig. 7 Measured contrasts of cold regions without and with material filter with LEGP collimator (negative sign of the contrast is ignored for the sake simplicity).

Discussion

Single photon emission computed tomography imaging systems use NaI(T1) scintillators for gamma photon detection and measurement. These scintillators have relatively poor energy resolution [36] compared to solid state (e.g. Germanium) detectors. In routine a 20% symmetrical energy window over the primary photopeak of the energy spectrum is adjusted. However, due to poor energy resolution a significant fraction, i.e., 30% to 40% reported by [37] and 20% to 40% investigated by [38] of photons measured in the standard energy window are in fact scattered photons. The variation in values of scatter fraction present in 20% symmetric energy window centered at 140 keV is due to the fact that the measured component of scattered gamma photons is dependent upon photon energy, source depth and size of the object. It increases as the depth of scattering medium is increased. The majority of scattered gamma photons lie in the lower part of the primary photopeak energy window since they are necessarily at lower energy. Kojima et al [39] investigated the distribution of low energy (scattered) gamma photons in the photopeak region by employing a 20% symmetrical energy window divided into a number of narrow energy windows and reported that 70-80% of the all scattered photons in the photopeak energy window (126 - 154 keV) is present in the region 126 - 139 keV.

In Tc-99m clinical imaging, only the data collected within the standard energy window (20%) over the photopeak is used for image reconstruction. Thus, much emphasis is given on the photopeak region of the Tc-99m spectra in terms of percentage reduction in relative count rate without and with material filter as compared to Compton continuum region. This study shows 12.61% decrease in count rate with material filter from photopeak region. Which is due to the attenuation of gamma photons (scattered and un-scattered), and also, to a smaller degree from the 1mm thick polythene sheets used to sandwich the Sn layer (for rigidity). In addition to that, the filter mount has a Pb frame which reduces the field of view and contributes to the reduction in count rate. It is not, however, unreasonable to suppose that at least some of this reduction results from the corresponding relative rejection of unwanted (scattered) gamma photons, whose presence would still be detected due to the poor energy resolution of the system.

Furthermore, analyzing the relative count rate results with the material filter as compared to without material filter 35% reduction corresponding to 60 – 125 keV gamma photon energies (part of spectrum) was observed. Nonetheless, in practice scattered gamma photons fall in this range are discriminated by electronic energy window. But, useful information can be extracted about the decrease of scattered gamma photons by drawing the line keeping in mind the trend of Compton continuum curve through the photopeak region (Fig. 3). Two dotted lines (without and with material filter) sketched all the way through the photopeak region (125 – 155 keV) represent the leakage of Compton scattered events. A noticeable reduction in the count rate with the

material filer has been observed. Moreover, it has been found that, in the region below 140 keV, i.e., 125 – 132 keV there is more reduction in the count rate as compared to the region above 132 keV up to 154 keV and that count rate can be related to the scattered gamma photon events shown in Fig. 8 (shaded region) that was plotted from the same data by normalizing the count rate at same peak. In addition, undoubtedly there is a possibility of a number of combinations of various order scattered events (single, double and triple) explained by [40] in computer simulated study that imitate the radioactivity concentration close to the clinical situations and as well as studied by [41] for a gamma camera having 10% energy resolution for 140 keV gamma photons. In another study conducted by [1] shows that the multiple-order scattered gamma photons within photopeak energy window data can be up to 20% of the total scatters. Furthermore, in Tc-99m imaging multiple order scatter into the photopeak region were investigated by [20, 37]. These types of events may reach at the surface of gamma camera crystal at a time on the same point and may produce a scintillation whose summed signal may fall within the standard energy window width, which in turn can be detected and registered in the image data. Such signals are the result of scattered gamma photon events with false positional information would cause the degradation of the quality of reconstructed image. Thus, prior to detection a substantial fraction of multiple - order scattered photons absorption can reasonably be assumed when the material filter is used. Further, results of this research show that the leakage of scattered photons into the photopeak energy window can be reduced by attaching material filter on the outer surface of a collimator, even when setting a standard energy window (20% centered at 140 keV).

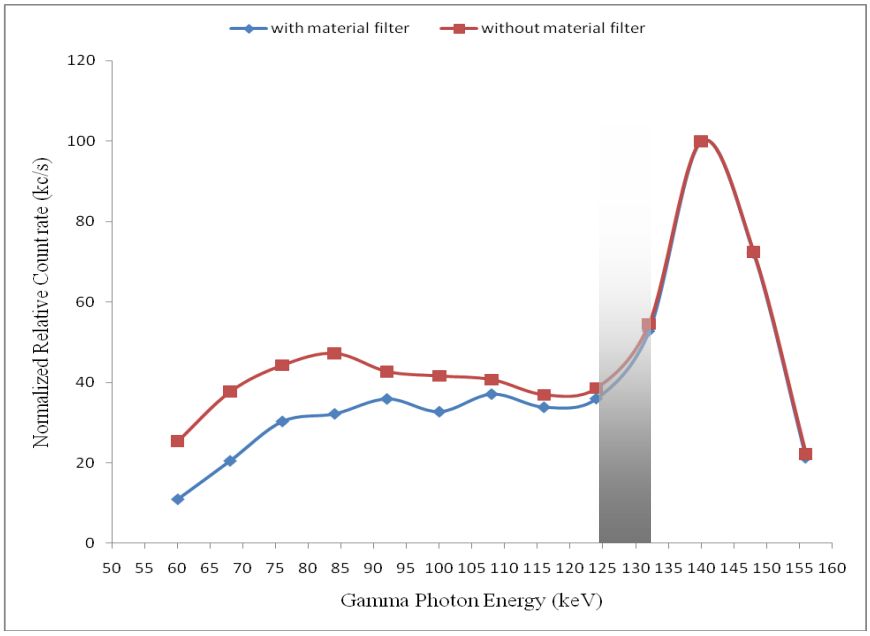

Fig. 8 Show the fractional absorption of various energy gamma photons (50 - 150 keV) by different materials (count rate normalized to same peak).

The results of the research reflect that material filter preferentially removes some fraction of scattered gamma photons prior to their detection; therefore, SPECT data are considered as scatter corrected. However, the material filter also attenuates some un-scattered gamma photons but that fraction could be comparatively smaller than the scattered gamma photons. As for as concerned the material filter induced scattered gamma photons, the filter was installed on the outer surface of collimator, thus, most probably some fraction of filter induced scattered gamma photons be stopped by the collimator before reaching the gamma camera scintillation detector. Moreover, the research conducted by [26] report that composite filter induced scatter has no degradation effect on image quality. In addition to that, this approach can be considered as preferred approach because correcting

the data before reconstruction of the image allows errors in the subsequent image to be reduced. In fact it was considered that some fraction of scatter component is removed by material filter from the projection data and it is well established that any little change in the raw data result the significant impact on image quality. Therefore, in this study image quality enhancement was expected with the use of material filter technique.

Measurement of %RMS noise is one of the indicators to assess the SPECT image quality. Material filter results show the significant decrease ($p<0.05$) in the %RMS noise as compared to without material filtered data image which reflects the removal of a fraction scattered gamma photons. As a matter of fact, presence of scattered photons in the image is considered as a noise factor [43].

Removal of scatter component using material filters from the ECT image data has been published by [26 – 28, 30, 42 - 43]. It is to be expected, from first principles, that a smaller cold region is more likely to be "filled in" by gamma photons scattered from the surrounding hotter regions, whereas only the edges of a larger cold region will be significantly affected. Thus, contrast improvement for smaller cold regions is expected to be better than for larger cold regions, as the results do, indeed, indicate. This observation is supported by the quantitative data presented in Fig. 7.

The results show the significant improvement in contrast of cold regions of diameter 7.3, 9.2 and 11.4mm at $p < 0.05$, but, statistically insignificant improvement for 5.9, 14.3 and 17.9mm diameter cold regions contrast when the material filter technique was used. Also enhancement of cold regions detectability and the distribution of counts in the background of the cold region appeared, on inspection, to be more uniform in the material filtered image. The expectation that at least image quality indicators, viz., %RMS noise, cold regions detectability and contrast can be improved has been established by direct measurement.

Conclusion

In conclusion, results of material filter technique show the reduction in scattered gamma photons prior to their registration in projection data. Thus, may be regarded as an on-line scatter reduction technique. Reduction in image noise, enhancement of cold regions detectability and contrast results indicate the utility of the material filter in Tc-99m SPECT. Therefore, for further tests of the technique are suggested on other phantoms which simulate the near realistic conditions as encountered in clinical studies.

Acknowledgement

Author gratefully acknowledges the Department of Nuclear Medicine, King's College Hospital, Denmark Hill, London, University of London. Dr Sidney Leeman and Mr Martin Clarke are thanked for valuable and helpful discussions and advice.

References

[1] B. F. Hutton, I. Buvat, and F. J. Beekman, "Review and current status of SPECT scatter correction," Phys Med Biol., vol. 56, pp. R85–R112, 2011.

[2] S. Liu, M. A. King, A. B. Brill, M. G. Stabin, and T. H. Farncombe, "Convolution-based forced detection Monte Carlo simulation incorporating septal penetration modelling," IEEE Trans Nucl Sci., vol. 55, pp. 967–74, 2008.

[3] J. Xiao, T. C. de Wit, W. Zbijewski, S. G. Staelens, and F. Beekman, "Evaluation of 3D Monte Carlo-based scatter correction for ^{201}Tl cardiac perfusion SPECT," J Nucl Med., vol. 48, pp. 637–44, 2007.

[4] E. Vandervoot, A. Celler, and R. Harrop, "Implementation of an iterative scatter correction, the influence of attenuation map quality and their effect on absolute quantitation in SPECT," Phy Med Bio., vol. 52, pp. 1527–1545, 2007.

[5] N. G. Sakellios, E. Karali, D. Lazaro, G. K. Loudos, and K. S. Nikita, "Monte Carlo simulation for scatter correction compensation studies in SPECT imaging using GATE software," Nucl Instr Meth Phy Res., vol. A569, pp. 404–408, 2006.
[6] A. Kojima, M. Matsumoto, S. Tomiguchi, N. Katsuda, Y. Yamashita, and N. Motomura, "Accurate scatter correction for transmission computed tomography using an uncollimated line array source," Ann Nucl Med., Vol. 18, pp. 45–50, 2004.
[7] M. K. Kyeong, V. Andrea, W. Hiroshi, S. Miho, F. Masahiro, B. I. Robert, and I. Hidehiro, "Contribution of scatter and attenuation compensation to SPECT images of nonuniformly distributed brain activities," J Nucl Med., vol. 44, pp. 512–519, 2003.
[8] A. Velidaki, K. Perisinakis, S. Koukouraki, J. Koutsikos, P. Vardas, and N. Karkavitsas, "Clinical Usefulness of Attenuation and Scatter Correction in Tl-201 SPECT Studies Using Coronary Angiography as a Reference," Hell J Cardiol., vol. 48, pp. 211-217, 2007.
[9] J. Xia, T. C. de Wit, W. Zbijewski, S. G. Staelens, and F. J. Beekman, "Evaluation of 3D Monte Carlo-Based Scatter Correction for ^{99m}Tc Cardiac Perfusion SPECT," J Nucl Med., vol. 47, pp. 1662-1669, 2006.
[10] J. Bai, J. Hashimoto, K. Ogawa, A. Kubo, A. Fukunaga, S. Onozuka, and K. Uchida, "Influence of photon scattering and attenuation on ROI analysis in brain perfusion single-photon emission tomography imaging of normal subjects," Ann Nucl Med., vol. 19, pp. 567–572, 2005.
[11] M. Noori-Asl, A. Sadremomtaz, and A. Bitarafan-Rajabi, "Evaluation of three scatter correction methods on estimation of photopeak scatter spectrum in SPECT imaging: A simulation study," Physica Medica 2004; http://dx.doi.org/10.1016/j.ejmp.2014.05.008.
[12] K. Okuda, K. Nakajima, M. Yamada, H. Wakabayashi, H. Ichikawa, H. Arai, S. Matsuo, J. Taki, M. Hashimoto, and S. Kinuya, "Optimization of iterative reconstruction parameters with attenuation correction, scatter correction and resolution recovery in myocardial perfusion SPECT/CT," Ann Nucl Med., vol. 28, pp. 60-68, 2014. DOI: 10.1007/s12149-013-0785-6.
[13] S. M. Hajizadeh, Oloomi Sh, P. Knoll, and H. Taleshi, "A new approach to scatter correction in SPECT images based on Klein_Nishina equation," Iran J Nucl Med., vol. 21, pp. 19-25, 2013.
[14] Oloomi Sh, E. H. Noori, R. Zakavi, P. Knoll, F. Kalantari, and S. M. Hajizadeh, "A New Approach for Scatter Removal and Attenuation Compensation from SPECT/CT," Iran J Basic Med Sci., vol. 16, pp. 1181-1189, 2013.
[15] R. G. Wells, K. Soueidan, R. Timmins, and T. D. Ruddy, "Comparison of attenuation, dual-energy-window, and model-based scatter correction of low-count SPECT to ^{82}Rb PET/CT quantified myocardial perfusion scores," J Nucl Cardiol., vol. 20, pp. 785-796, 2013. DOI: 10.1007/s12350-013-9738-7.
[16] J. C. Erhardt, and L. W. Oberley, "Effects of spectral changes on scanning," Radiology., vol. 104, pp. 207 – 208, 1972.
[17] P. Msaki, B. Axelsson, C. M. Dohl, and S. A. Larsson, "Generalised Scatter correction method in SPECT using point scatter distribution functions," J Nucl Med., vol. 28, pp. 1861 -1869, 1987.
[18] J. Mas, P. Hannequin, Y. R. Ben, B. Bellaton, and R. Bidet, "Scatter correction in SPECT by constrained factor analysis of dynamic structures (FADS)," Phy Med Bio., vol. 35, pp. 1451 – 1465, 1990.
[19] S. D. Egbert, and R. S. May, "An Integral-Transport for Compton scatter correction in emission computed tomography," IEEE Trans Nucl Sci., vol. 27, pp. 543 – 548, 1980.
[20] C. E. Floyd, R. J. Jaszczak, C. C. Harris, and R. E. Colman, "Energy and spatial distribution of multiple order Compton scatter in SPECT: A Monte Carlo investigation," Phy Med Bio., vol. 29, pp. 1217 – 1230, 1984.
[21] M. A. King, G. J. Hademenos, and S. J. Glick, "A dual-photopeak window method for scatter correction," J Nucl Med., vol. 33, pp. 605-612, 1992.
[22] D. J. Waggett, and B. C. Wilson, "Improvement of scanner performance by subtraction Compton scattering using multiple energy windows," Br J Radiology., vol. 51, pp. 1004 – 1010, 1978.
[23] J. M. Sanders, and N. M. Spyrou, "Improvement of image quality in emission and transmission tomography by reduction of scattered photons," Nuclr Instr Meth Phys Research., vol. 221, pp. 93 -97, 1984.

[24] R. J. Jaszczak, K. L. Greer, C. E. Floyd, C. C. Harris, and R. E. Colman, "Improved SPECT quantification using compensation for scattered photons," J Nucl Med., vol. 25, pp. 893 – 900, 1984.
[25] P. H. Pretorius, A. J. van Rensburg, A. V. Aswegen, M. G. Lotter, D. E. Serfontein, and C. P. Herbst, "The channel ratio method of scatter correction for radionuclide quantitation," J Nucl Med., vol. 34, pp. 330 – 335, 1993.
[26] G. Muehllehner, and R. J. Jaszczak, "The Reduction of Coincidence Loss in Radionuclide Imaging Cameras through the Use of Composite Filters," Phy Med Bio., vol. 19, pp. 504-510, 1974.
[27] M. Pillay, B. Shaprio, and P. H. Cox, "The effect of an alloy filter on gamma camera images,' Eur J Nucl Med., vol. 12, pp. 293-295, 1986.
[28] M. Pillay, and R. S. Manon, "Filter for Gamma Ray Camera," US Patent., 4,852,142, 1989.
[29] K. R. Pollard, A. N. Bice, J. F. Eary, L. D. Durack, and T. K. Lewellen, "A method for imaging therapeutic doses of Iodine-131 with a clinical gamma camera," J Nucl Med., vol. 33, pp. 771-776, 1992.
[30] T. J. Spinks, S. I. Shah, "Effect of lead filters on the performance of a neuro-PET tomograph operated without septa," IEEE Trans Nucl Sci., vol. 40, pp. 1087-1091, 1993.
[31] S. I. Shah, "Reduction of Scattered Gammas and Attenuation Correction in Tc-99m SPET Imaging," PhD Thesis University of London, UK, 1996.
[32] Goodfellow Metals Limited, "Metals and Materials for Research and Industry," Cambridge Science Park Cambridge, England, 1994.
[33] W. S. Rasband, "ImageJ," U. S. National Institutes of Health, Bethesda, Maryland, USA, 1997-2015. http://imagej.nih.gov/ij
[34] K. Greer, "SPECT Phantom User's Manual DSC-5000-RO2," Data Spectrum Corporation, Chapel Hill USA, 1983.
[35] L. T. Chang, "A method for attenuation correction in radionuclide computed Tomography," IEEE Trans Nucl Sci., vol. 35, pp. 638-643, 1978.
[36] S. A. Larsson, B. Axelsson, C. M. Dahl, and P. Msaki, "The use of 1-D and 2-D scatter deconvolution techniques for contrast enhancement and quantification in SPECT," J Nucl Med., vol. 27, pp. 884, 1986.
[37] A. Kojima, M. Masanori, and T. Mutsumasa, "Experimental analysis of scattered photons in Tc-99m imaging with a gamma camera," Ann Nucl Med., vol. 5, pp. 139-144, 1991.
[38] M. Ljungberg, and S. E. Strand, "A Monte Carlo program for the simulation of scintillation camera characteristics," Comput Methods Programs Biomed., vol. 29, pp. 257-272, 1989.
[39] W. P. Segars, D. S. Lalush, and B. M. W. Tsui, "A realistic spline-based dynamic heart phantom," IEEE Trans. Nucl. Sci., vol. 46, pp. 503–506, 1999.
[40] K. W. Logan, and W. D. McFarland, "Single photon scatter compensation by photopeak energy distribution analysis," IEEE Trans Med Imaging., vol. 11, pp. 161-164, 1992.
[41] C. E. Floyd, R. J. Jaszczak, C. C. Harris, K. L. Greer, and R. E. Colman, "Monte Carlo evaluation of Compton scattered subtraction in single photon emission computed Tomography," Med Phys., vol. 12, pp. 776–778, 1985.
[42] R. Boellaard, H. W. A. M. de Jong, C. F. M. Molthoff, F. Buijs, M. Lenox, R. Nutt, and A. A. Lammertsma, "Use of an in-filed-of-view shield to improve count rate performance of a single crystal layer high-resolution research tomograph PET scanner for small animal brain scans," Phys Med Biol., vol. 48, pp. N335-N342, 2003.
[43] D. C. Ficke, and M. M. Ter-Pogossian, "Hardening of annihilation radiation for improved coincidence detection in PET," Conference record. IEEE Medical Imaging Conference., pp. 1303-1304, 1990.